Geometrical Factor of Conductivity in Rocks:

BRINGING NEW RIGOR TO A MATURE MODEL

Carl Fredrik Berg*, David Herrick†, David Kennedy‡

This paper was prepared for presentation at the SPWLA 57th Annual Logging Symposium held in Reykjavik, Iceland June 25-29, 2016.

ABSTRACT

Recurrent themes can be found in the history of mathematics and physics, and science in general, among them the development of ideas from intuitive concepts and qualitative arguments that are at a later date validated by subsequent, more rigorous, analysis. Indeed, many times it has been the empirical success of a qualitatively justified theory that has motivated the development of more rigorous methods.

So has it been with the development of a conductivity theory for petroleum reservoir rocks. Like Newton when declining to expound on the cause of gravity ("*Hypotheses non fingo*"), Archie makes no hypothesis as to reason for the success of his functions relating water saturation to porosity, brine resistivity, and bulk rock resistivity. Excepting a few attempts in the 1950s, serious investigation into the physics of conduction in rocks did not begin until 40 years following Archie's seminal work. These second attempts at explanations were based upon effective media theories, but when applied to rocks these are approximations, and have not led to "first principles" models.

D. C. Herrick and W. D. Kennedy (1993) proposed a model stating: "The conductivity σ_t, of a water-bearing rock composed of non-conducting minerals, and which may contain hydrocarbons displacing some of the original water from its intergranular pore-space, is a function of the conductivity of the conducting phase (usually brine) σ_w, porosity ϕ, fractional volume occupied by the conducting phase ϕS_w, and spatial distribution, or geometry, of the conducting phase; i.e., $\sigma_t = f(\sigma_w, \phi, S_w, \text{geometry})$." As a functional form they proposed $\sigma_t = \sigma_w \phi S_w E_t$ with E_t being an explicit geometrical factor intended to account for the effects of the brine geometrical distribution upon bulk rock conductivity.

In 2012, C. F. Berg published an article "Re-examining Archie's law: Conductance description by tortuosity and constriction". Berg, beginning with infinitesimal elements of conducting brine volume, integrates these elements into tortuosity and constriction factors describing the conductance of the porous medium.

In this paper we show that the combined effect of the tortuosity and constriction factors developed by Berg is identical to the geometrical factor E_t of Herrick and Kennedy. The convergence of these results puts the geometrical factor theory on a rigorous analytical footing, moving theoretical petrophysics past raw empiricism to analytical rigor.

INTRODUCTION

History

The estimation and understanding of electrical conductivity in porous media has many applications in science and technology. An important use is estimation of hydrocarbon reserves based upon the responses of logging instruments in wells drilled for oil or gas production. The accuracy of the estimation depends upon two factors: (1) the quality of the porosity and resistivity estimates, and (2) the efficacy of the model used to convert porosity and resistivity into estimates of fluid saturation for use in determining petroleum reserves.

The first oil well surveyed for formation resistivity was in Pechelbronn, France on September 5, 1927. The spontaneous potential (SP) was discovered soon after. The first suite of log curves was the combination of the SP deflection and formation resistivity responses. A combination of high apparent resistivity and low SP could be correlated with petroleum bearing formations, but it might also indicate brine-filled formations having low porosity. Thus, logs were qualitatively useful, but still without quantitative predictive capabilities.

There was no quantitative interpretation of formation resistivity in terms of brine saturation until 1941. Attempts to understand formation resistivity quantitatively began in the mid-1930s. Between 1936 and 1938 four studies were published (Wyckoff and Botset, 1936; Jakosky and Hopper, 1937; Leverett,

* Statoil
†Yellowstone Petrophysics LLC
‡QED Petrophysics LLC

1938; Martin, Murray, Gillingham, 1938) studying the relationship between the bulk resistivity R_t of a rock sample to the fractional brine volume S_w in its pore space. The bulk resistivity R_t was parameterized as the *resistivity index* R_t/R_0, dividing the resistivity R_t of a sample by R_0 the resistivity of a fully brine-saturated sample. The primary concern of these authors had been the relationship between permeability and porosity. It was left to G. E. Archie in 1942 to notice that these authors had independently recorded essentially the same relationship between fractional brine saturation S_w and the resistivity index, namely, a power law: $R_t/R_0 \equiv S_w^{-n}$. By convention the *saturation exponent* n is taken to be a positive number, with its value typically approximately equal to 2.

In the same paper Archie introduced the *formation resistivity factor*, the ratio of the resistivity R_0 of the brine-saturated sample to the resistivity R_w of the brine in the pore volume, $F = R_0/R_w$. Archie also observed that the relationship between the formation resistivity factor and the sample porosity ϕ could be estimated by a power law, viz. $F = R_0/R_w \equiv \phi^{-m}$. By convention m is a positive number; Archie observed that m typically was in a range of 1.8 to 2.

Combining these two power-laws gives what is commonly referred to as *Archie's law*: $R_t = a\,R_w\phi^{-m}S_w^{-n}$. Here it has become customary to include an additional fitting parameter a, (first introduced by Owens, 1952). The physical interpretations of bulk resistivity R_t, brine resistivity R_w, porosity ϕ, and water saturation S_w are obvious. Note that as there is no information on the geometrical distribution of the conducting phase in these parameters, thus the electrical effects of the conducting phase geometry must be contained in the remaining parameters m, n and a. There has been a significant effort to attribute physical significance to these parameters, which has led to the commonly used names of *cementation exponent* for m (Guyod, 1944) and *tortuosity factor* for a (Schopper, 1966). However, there is no argument based upon physical first principles that links cementation with m, nor tortuosity with a; these relationships (and corresponding misnomers) are based solely on correlations.

Archie did not predict these relationships through an analysis from first principles; he merely selected power law fits to observed data. It is thus an empirical law, as there is no *a priori* physics in the Archie equation. Regardless that Archie's law is merely an empirical model for the rocks in his data set, it is reasonable that it should work for similar rocks. Indeed, for a restricted class of rocks, the Archie law works very well. Rocks where the porosity-conductivity relationship is adequately described by Archie's model are called *Archie rocks.* Such Archie rocks are typically sandstones without a microporous phase (e.g. without clays) and with a small grain size variation, giving a simple intergranular pore system. Due to its wide applicability and simplicity, the Archie model was quickly and universally adopted, and it remains in use to this day.

There have been later attempts to derive Archie's law from first principles. It was shown by Sen et.al. (1981) that Archie's law follows from the work of Bruggeman and Hanai, however this is only applicable to non-conductive particles dispersed in a conductive matrix. The original work of Bruggeman and Hanai considered dispersed spheres, which would give $m = 3/2$, which is comparable to experimental results for fused spherical glass beads (Sen, 1981). Even though the derivation only holds for dispersed particles, the equation has been applied to immersed networks of interconnected particles in addition to dispersed individual particles (e.g., Bussian, 1983).

It is thus possible to deduce something similar to Archie's law from an effective medium approximation, or mixing rule, for relatively simple porous media. Unfortunately, the models used are hardly representative of rocks. There is therefore no physical explanation for the parameters used in the Archie model. Even the relatively common case of anisotropic rocks cannot be explained by Archie's law; the adjustable parameters are scalars. Due to the lack of physical basis for the Archie formula, the adjustable parameters have merely been correlated to rock properties. Efforts to characterize the parameters used in the Archie model in terms of rock properties has been ongoing since Archie's work (Guyod, 1944) and is still ongoing today (Montaron and Han, 2009; Glover, 2009).

Even though the Archie model has a proven record of solving problems related to the conductivity of rocks, the lack of physical basis and thereby lack of physical interpretation of the adjustable parameters motivates the search for an alternative theory. The formation factor has been described by first principles, where the effective conductance is formulated as an integral of the microscopic electrical potential (Johnson et al., 1986). A similar formulation was independently proposed by Herrick and Kennedy (1994). Further, by extending the results to fractional brine saturations, they formulated a complete alternative theory to Archie's law. Herrick and Kennedy (2009) call their model *the geometrical factor theory;* and it is restated below for completeness.

The physical explanation for the parameters in the proposed theory was alluded to in the original paper (Herrick and Kennedy, 1994), where it was substantiated that the geometrical factor represented the tortuosity and constrictions of the pore structure. This physical explanation was confirmed by Berg (2012). Berg integrated infinitesimal elements of conducting brine volume elements into tortuosity and constriction factors, the combined effect of the tortuosity and constriction factor gives the geometrical factor.

Berg's model provides a complete theory for electrical conductance in rocks based on first principles, where the parameters are firmly linked to the pore structure of the rock.

The geometrical factor theory (GFT)

A reservoir rock can be considered as comprising a conductive phase (brine) and possibly several non-conductive phases. The non-conductive phase is typically the matrix of the rock, e.g. quartz grains, and, if present, also non-conductive fluids such as oil and/or gas that partially fill the pore-space of the rock. The conductive phase is primarily an electrolyte (brine). Reservoir rocks often contain other conductive phases, such as mineral surfaces, clays and metallic sulphides, commonly pyrite. For simplicity we will assume a single conductive phase (brine) filling (or partially filling) the pore space, with constant conductivity σ_w.

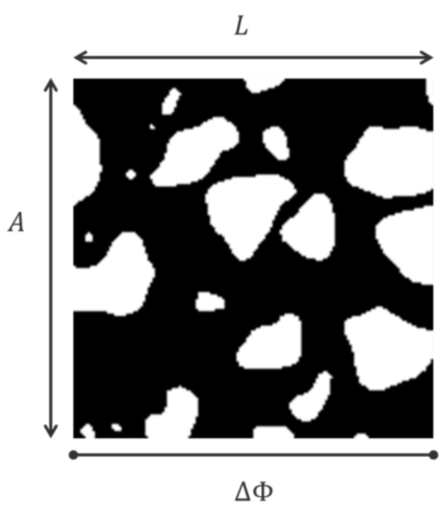

Figure 1. A 2-D cross-section resembling a rock sample, with pore space Ω in black and rock matrix in white. The sample has length L with a potential difference of $\Delta\Phi$ applied between the vertical sides of the sample. This 2-D model is based on a rock sample, however the irregular grains have been separated from each other to permit through-going continuity of the conductive fluid phase required to illustrate conduction in a 2-D model.

We will therefore consider a rock sample of volume V consisting of an insulating matrix and possibly an insulating fluid partially filling the pore space, together with an electrolyte (brine) filling the remaining pore volume Ω in the model. The sample has a length L in direction of an applied potential difference $\Delta\Phi$ over the side planes, and the sample has a constant cross-sectional area of size A. For illustration purposes, we have created a two-dimensional model resembling a rock sample, as depicted in Figure 1. This model is based on a cross-section of a rock sample; however, we have eroded the matrix significantly to increase the connectedness in the plane. The constant voltage drop $\Delta\Phi$ leads to a direct current.

Inside the electrolyte, the current density $\mathbf{J}$ is given by Ohm's law as $\mathbf{J} = \sigma_w \mathbf{E}$, where $\mathbf{E}$ is the electrostatic field. The electrostatic field $\mathbf{E} = \nabla\Phi$ is the gradient of the electrical potential Φ. Change of electric charge in any volume equals the amount of charge flowing into the volume minus the amount of charge flowing out. At a point, the change of electric charge is given by the divergence of the current density $\nabla \cdot \mathbf{J}$. At steady state we have constant charge everywhere, giving $\nabla \cdot \mathbf{J} = 0$. Combining the equations above implies that the electrical potential must satisfy the Laplace equation

$$\sigma_w \nabla^2 \Phi = \nabla \cdot \sigma_w \nabla \Phi = \nabla \cdot \sigma_w \mathbf{E} = \nabla \cdot \mathbf{J} = 0, \qquad (1)$$

with the boundary condition $\Phi = \Phi_{in}$ on the left and $\Phi = \Phi_{out}$ on the right. Electric current cannot flow into or out of any nonconductive phase, therefore the current must flow parallel to the interface between the conductive phase (brine) and the non-conductive phase (matrix).

Solving the equation above for the pore space in Figure 1, we get a solution for the potential Φ as depicted in Figure 2. We have used the boundary conditions $\Phi_{in} = 1$ on the left and $\Phi_{out} = 0$ on the right. In Figure 3 we have a plot of the magnitude of the electrostatic field $\|\mathbf{E}\| = \|\nabla\Phi\|$, illustrated by the color spectrum varying from a high field (red) to low (blue) with the intermediate spectrum denoting the continuous variation in the field. The electrostatic field determines the current density distribution making Figure 3 also a map of the amount of electric current flowing at each point. The current density varies from the lowest values

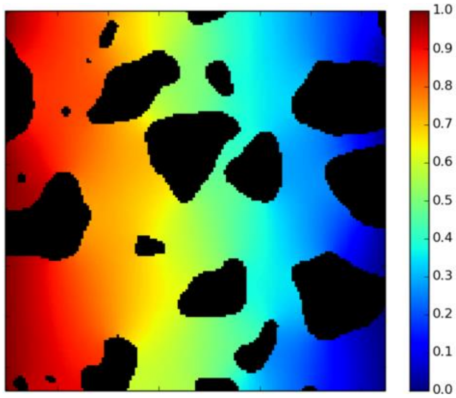

Figure 2. Plot of the potential field $\mathbf{\Phi}$ inside the pore space obtained by solving the Laplace equation. The potential is set equal 1 on the left and 0 on the right.

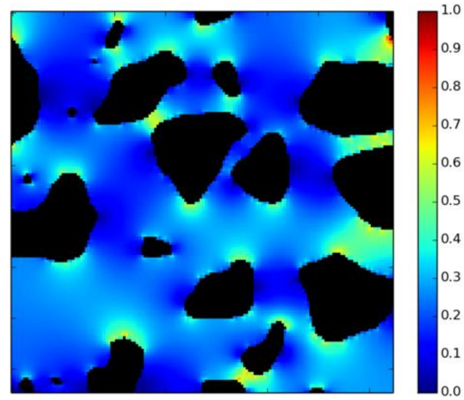

Figure 3. Plot of the magnitude of the normalized electrostatic field $\|\mathbf{E}\| = \|\mathbf{\nabla\Phi}\|$ inside the pore space.

in blue through the spectrum to the highest values of current density in red. The lowest current density occurs in the middle of the large pores and the highest current densities are in the smallest constrictions. In the mental analogue of a stream flowing through boulders, the flow rate would be represented by Figure 3.

Consider now the power developed in the conducting phase. The total power developed is given by

$$P = \int_\Omega \mathbf{J} \cdot \mathbf{E}\, dV = \int_\Omega \sigma_w \nabla\Phi \cdot \nabla\Phi\, dV \\ = \int_\Omega \sigma_w \|\nabla\Phi\|^2\, dV. \qquad (2)$$

At the same time, the total power is given by the product of total current I and applied voltage drop $\Delta\Phi$. This gives the following expression for the total current:

$$I = \frac{1}{\Delta\Phi}\int_\Omega \sigma_w \|\nabla\Phi\|^2\, dV. \qquad (3)$$

By definition, the effective conductivity of our sample is $\sigma_t = (I/A)/(\Delta\Phi/L) = (I/\Delta\Phi)/(L/A)$. For a partially brine filled rock sample, we denote the fractional volume of the conducting phase Ω as $\Omega/V = \phi S_w$. This gives the following expression:

$$\frac{R_w}{R_t} = \frac{\sigma_t}{\sigma_w} = \frac{IL}{\sigma_w \Delta\Phi A} = \frac{L}{A\|\Delta\Phi\|^2}\int_\Omega \|\nabla\Phi\|^2\, dV \\ = \phi S_w \frac{1}{\Omega}\int_\Omega \frac{\|\nabla\Phi\|^2}{\|\Delta\Phi/\mathrm{L}\|^2}\, dV \\ = \phi S_w E_t, \qquad (4)$$

where the last part of the expression is equivalent to the factor E_t. This can be expressed similarly to Archie's law as $R_t = \phi^{-1} S_w^{-1} E_t^{-1} R_w$, or reciprocally as $\sigma_t = \phi S_w E_t \sigma_w$. Assuming a fully water-saturated sample, $S_w = 1$, we then get the following expression for the *formation conductivity factor* f:

$$f = F^{-1} = \frac{R_w}{R_0} = \frac{\sigma_0}{\sigma_w} = \phi E_0, \qquad (5)$$

where E_0 is denoting the factor E_t for a fully water-saturated sample. This expression of the formation factor was derived in Johnson, et al. (1986). Independently, this was later generalized to the equivalent of Archie's law in (Herrick and Kennedy, 1994). Following (Kennedy and Herrick, 2012) we define E_t and E_0 as the *geometrical factor*[1] which accounts for the reduction in conductance due to the geometric distribution of the non-conductive phase. The geometrical factor is the building block of the geometrical factor theory. As shown above, the

[1] It should be noted that E_t is denoted as *electrical efficiency* by Herrick and Kennedy (1994) and *conductance reduction factor* by Berg (2012).

geometrical factor is deduced from first principles.

Let us start by considering the case of a completely water saturated rock sample, $S_w = 1$, which gives the following equation:

$$\sigma_0 = \sigma_w \phi E_0 \qquad (6)$$

Unlike Archie's equation, this formula has the advantage of being intuitive; the bulk conductivity of the rock sample is proportional to the conductivity of the brine in the sample σ_w, proportional to the amount of brine in the sample ϕ, and a proportionality constant E_0 that depends upon (and quantifies) effects of the pore geometry. As the minimum bulk conductivity that a rock can have is zero, while the maximal conductivity is $\sigma_w \phi$, the geometrical factor E_0 must lay between 0 and 1.

Each rock sample is characterized by its geometrical factor E_0, and it can be evaluated using the measureable quantities σ_0, σ_w and ϕ;

$$E_0 = \frac{\sigma_0}{\sigma_w \phi}. \qquad (7)$$

There is no *a priori* reason for a correlation between porosity and the geometrical factor. Archie observed that there is a power-law correlation between the porosity and the formation factor, as given by the cementation exponent. If the correlation between the formation resistivity factor and porosity was perfectly described by a power-law, this would imply a functional relationship between porosity and geometrical factor too. Thus a suite of Archie rocks, i.e., rocks exhibiting a strong correlation between porosity and formation resistivity factor, implies a correlation between porosity and the geometrical factor. Conversely; little correlation between the porosity and the geometrical factor implies we do not have a suite of Archie rock samples.

Using Archie's cementation exponent, $\phi^m = f = F^{-1} = \phi E_0$, we get $E_0 = \phi^{m-1}$. Using a typical value for the cementation exponent of 2, this gives $E_0 = \phi$. Thus the correlation observed by Archie indicates there is a relation between E_0 and ϕ in a typical suite of Archie rocks; further E_0 is expected to be approximately equal in value to ϕ. In general, as porosity is changed, the pore geometry simultaneously changes. However what are the detailed petrologic changes which result in a particular value of E_0? Very little information is available to answer this important question, suggesting a whole new area of research.

Partially saturated porous media

Now consider a rock partially filled with brine, i.e. $S_w < 1$. In the equation deduced above we have $\sigma_t = \phi S_w E_t \sigma_w$, where ϕS_w is the fractional brine volume conducting electricity. In the reciprocal of Archie's law, $\sigma_t = a^{-1}\, \phi^m S_w^n \sigma_w$, both the porosity and saturation are raised to a power. In this form, a weakness of the Archie formulation is apparent: The fractional brine volume ϕS_w in the rock has its own unique pore geometry, and logically it should be treated as a single entity. However, ϕS_w is not treated as a single entity in the Archie model; the factors are treated separately as the result of having been put together from two separate experiments, one using water saturation at fixed porosity and the other using porosity at fixed water saturation (i.e., $S_w = 1$).

Following the example of Archie, we distinguish the geometrical factor E_0 for the fully brine saturated rock from the geometrical factor E_t for the partially brine saturated rock. To isolate the modification of the brine geometry due to the emplacement of a hydrocarbon phase we normalize the geometrical factor of the hydrocarbon-bearing rock by dividing by the geometrical factor of the same rock when fully brine saturated. The quotient, denoted $e_t = E_t/E_0$, is then a factor describing the distribution of brine that shares the pore space with hydrocarbons. Replacing E_t by the components $E_0 e_t$, we get the equation

$$\begin{aligned} \sigma_t = \phi S_w E_t \sigma_w &= (\phi S_w)(E_0 e_t)\sigma_w \\ &= (E_0 \phi)(e_t S_w)\sigma_w, \end{aligned} \qquad (8)$$

where possible groupings of the factors are highlighted using parenthesis. The last grouping follows the logic of the traditional Archie equation. Then the factor e_t should correlate to water saturation S_w; as brine is displaced by hydrocarbons, the brine geometry and thereby e_t changes.

GFT theory applied to Fontainebleau sandstone

Let us now apply the theory described above to a set of Fontainebleau sandstone data from Jacquin (1964). The Fontainebleau sandstone consists of quartz grains of around $200\mu m$ in diameter, with porosities ranging from 3% to 30% due to quartz cementation. The simplicity of this sandstone should make it an Archie rock.

In Figure 4 we have plotted the geometrical factor versus porosity. As discussed above, a cementation exponent of 2 implies a linear 1:1 relationship between porosity and the geometrical factor. The coefficient of determination for a linear fit to the data is 0.69, so there is indeed a linear correlation between the porosity and the geometrical factor. However, the relationship between the porosity and the geometrical factor might be described as well by non-linear correlations in the case of the Fontainebleau sandstone. The scatter in the data precludes any definite conclusion about the best correlation to describe the geometric factor-porosity relationship. After acknowledging measurement errors, a scatter of this sort implies that the sample suite is somewhat heterogeneous; i.e., the samples experienced differences in their geologic evolution in addition to varying degrees of a single formative geologic process which relates them.

As porosity ϕ and the geometrical factor E_0 are both components of the formation conductivity factor, $f = \phi E_0$, there is an autocorrelation between the porosity ϕ or the geometrical factor E_0 and their product $f = \phi E_0$. For this reason one always observes a stronger correlation between the porosity ϕ and the formation conductivity factor f (or the formation resistivity factor F) than between the porosity ϕ and the geometrical factor E_0. This is clearly seen in the plot in Figure 5, which has a coefficient of determination of 0.959 for a linear fit to the f vs. ϕ data. The same autocorrelation is seen in f vs. E_0 correlations. One always observes a stronger correlation between f and E_0 and between f and ϕ than between the porosity ϕ and the geometrical factor E_0. However, the f vs. ϕ or E_0 correlations include the autocorrelations pointed out above, but they do not contain any more information about the rocks under consideration than that in the correlation between the geometrical factor and the porosity. Quite the contrary, the autocorrelation obscures the underlying correlation between the geometrical factor and the porosity, if any.

Another example of how this autocorrelation works is witnessed in the set of consolidated sandstone cores from the Gulf coast plotted in Figure 6 and used by Archie (1942). We have a fair correlation between the formation conductivity factor and porosity, giving a coefficient of determination of 0.74 as seen in Figure 7. However, the geometrical factor versus porosity plotted in Figure 6 gives a coefficient of determination of 0.29. Thus the linear correlation between the porosity and the geometrical factor is weak. In contrast with the Fontainebleau samples considered earlier, the Gulf coast samples do not share geologic history as they were from different locations, fields, depths and formations. One would therefore expect a weaker (if any) correlation between geometrical factor and porosity for the Gulf coast samples compared to the Fontainebleau samples. Such correlation differences between sample sets are obscured by the inherit autocorrelation when comparing the formation conductance/resistivity factor to porosity.

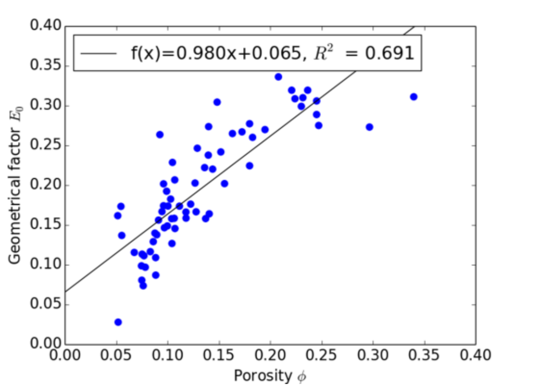

Figure 4. Plot showing the geometrical factor versus porosity for the data from Jacquin (1964).

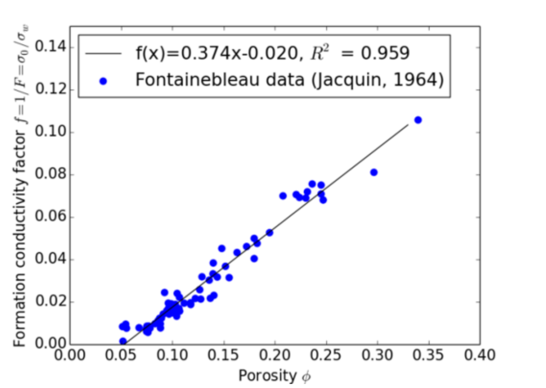

Figure 5. Plot of porosity versus the formation conductivity factor f, together with a linear fit to the data.

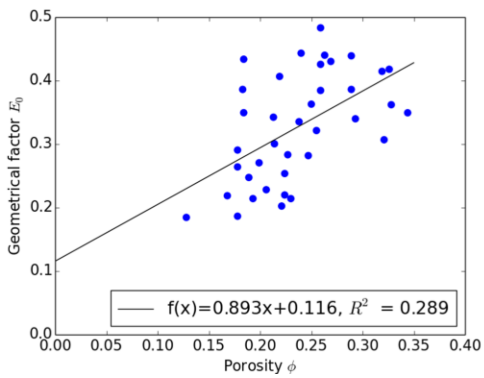

Figure 6. Plot showing the geometrical factor versus porosity for the set of consolidated sandstone cores from the Gulf coast, used in Archie (1942).

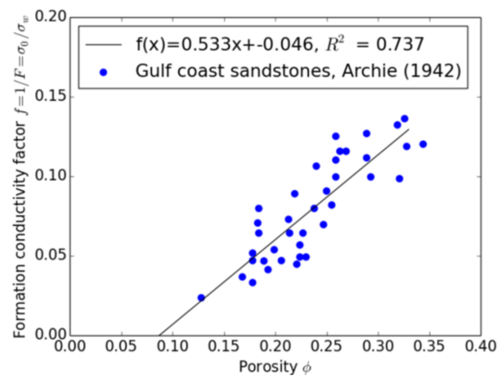

Figure 7. Plot of porosity versus the formation conductivity factor $\boldsymbol{f}$, together with a linear fit to the data.

Description of the geometrical factor

The geometrical factor E_0 is dependent on the pore geometry and has no intrinsic relationship to porosity. One well known geometrical descriptor is the tortuosity. Returning to the 2-D pore structure introduced earlier, the direction of the electrostatic field $\mathbf{E} = \nabla\Phi$ is indicated by vectors in Figure 8. This gives the direction of the current, and tracking the current through the medium gives rise to electric field lines as indicated in Figure 9. Note that this visualization is not complete in the sense that every point in the model lies upon a unique field line whereas only a representative subset of the field lines can be illustrated. The field lines are continuous; all start on the left side and end on the right side of the figure.

The actual length L_Γ of an electric field line Γ inside the pores of our rock sample is longer than the length of the rock sample L. In other words, the electric field line is tortuous, and the magnitude is described by the *tortuosity*[2] $\tau(\Gamma) = L_\Gamma/L$ of the field line Γ. As the electric field line is always longer than the length of the sample, the tortuosity is a number larger than 1. A larger tortuosity value indicates a more tortuous, i.e., longer, electric field line.

[2] There is no consensus on how tortuosity should be defined, see e.g. Clennell (1997) for an overview. Other common definitions include $(L_\Gamma/L)^2$ (see e.g. (Wyllie and Rose 1950)), and the reciprocally L/L_Γ (see e.g. (Bear 1988)).

The applied potential $\Delta\Phi$ divided by the length of the field line L_Γ gives the average magnitude of the electric field along the streamline; $\|\mathbf{E}\| = \Delta\Phi/L_\Gamma$. This gives an interstitial current density $\|\mathbf{J}\| = \sigma_w\|\mathbf{E}\| = \sigma_w\Delta\Phi/L_\Gamma$, thus increased tortuosity reduces the interstitial conductivity of the porous medium.

This correspondence between the length of the field lines and the interstitial current was first noted by Kozeny, then in the setting of fluid flow. Building on the work of Kozeny, Carman noted that the average interstitial current density $\mathbf{J}_x$ in direction x of the applied potential equals $\|\mathbf{J}_0\|/\phi$, where $\|\mathbf{J}_0\| = \sigma_0\Delta\Phi/L$ is the effective current density for the porous medium. The interstitial current density $\mathbf{J}$ is related to the interstitial current density in direction of the applied potential $\mathbf{J}_x$ by a factor of $\|\mathbf{J}\|/\|\mathbf{J}_x\| = L_\Gamma/L = \tau$, thus the average interstitial current density $\|\mathbf{J}\| = \sigma_w\Delta\Phi/L_\Gamma$ equals $(\|\mathbf{J}_0\|/\phi)\,(L_\Gamma/L) = (\sigma_0/\phi)\,(\Delta\Phi/L)\,(L_\Gamma/L)$. This reduces to the Kozeny-Carman equation reformulated to electrical conductance:

$$\sigma_0 = \sigma_w\phi\tau^{-2}. \tag{9}$$

Considering a single cylindrical tube of length L' as depicted in Figure 10. The volume of the tube will be $\tau = L'/L$ larger than a tube with equal cross-sectional area of length L. At the same time, the local current density $\|\mathbf{J}\| = \sigma_w\Delta\Phi/L'$ will be $\tau = L'/L$ smaller than the local current density $\|\mathbf{J}\| = \sigma_w\Delta\Phi/L$ in a tube of length L. So the tortuous tube has increased the volume and decreased the conductance by the same factor

$\tau = L'/L$. The combined effect of change in volume and conductance renders the tortuosity as squared in equation (9).

Visual inspection of Figure 9 reveals that in this simplified 2-D example the tortuosities for the streamlines are close to 1. It can be shown that for a cubic sphere pack the tortuosity is approximately $\pi/2$. For simple granular porous media the tortuosity is often in the same range as for the sphere pack, in the range 1 to 2. However, rocks exist, that have significantly higher tortuosity values, e.g., sandstones with large amounts of quartz cementation.

From the geometrical factor theory introduced above we have the equation $\sigma_0 = \sigma_w \phi E_0$ (equation (6)). From equation (9), this would imply $E_0 = \tau^{-2}$. As seen in Figure 4, the geometrical factor E_0 approaches zero for low porosities. On the other hand, as the electric field is smooth and the porous medium is finite, the tortuosity τ cannot approach infinity for low porosities. Thus the geometrical factor E_0 must be controlled by more than the tortuosity alone. As pointed out by Owen (1952), the constricting nature of porous media also limits the current flow. For sandstones the pore space can be loosely divided into pore bodies being the larger space between the grains, while the more narrow spaces connecting the pore bodies are called pore throats. The current will then sequentially pass through pore bodies and pore throats. As the conductance is proportional to the cross-sectional area, the variation in cross-sectional area between the pore bodies and pore throats will limit the current. That the magnitude of the electrical field is larger in the pore throats than in the pore bodies is typically more pronounced in three dimensions than in two, still this effect can be seen in Figure 8b. Close to the right boundary in Figure 8 the cross-section contains more of the non-conductive matrix, thus there is less of the conductive phase and the magnitude of the electric field becomes larger.

Returning to a simple pore volume model consisting of a single cylindrical tube is again instructive: We now assume the tube has varying cross-sectional area of $A(x)$ at a distance x along the tube of total length L as illustrated in Figure 11. As the conductance is proportional to the cross-sectional area, the resistance is inversely proportional to the cross-sectional area. The total resistance along the tube is then the integral of the local resistance:

$$R_t = \int R(x)dx = \rho \int \frac{1}{A(x)} dx, \qquad (10)$$

where $R(x)$ is the resistance at a distance x along the tube, and $A(x)$ is the cross-sectional area at the same point. The smallest pore throats have the highest resistance and tend to dominate the integral. If the tube has length L, then a tube of equal resistance, but with constant cross-sectional area would then have a cross-sectional area of:

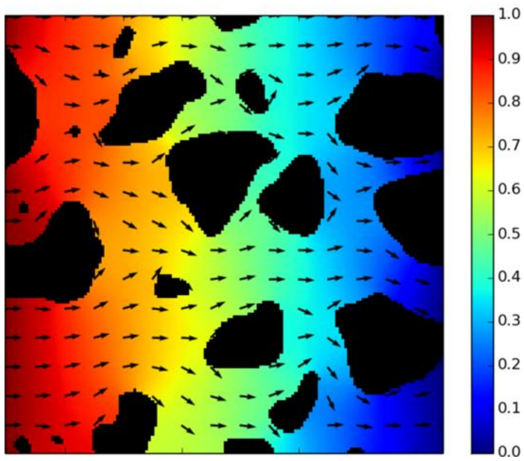

Figure 8. Arrows indicating the direction of the electric field $\mathbf{E} = \nabla\mathbf{\Phi}$, where the colors show the underlying electrical potential $\mathbf{\Phi}$. The potential is 1 on the left and 0 on the right.

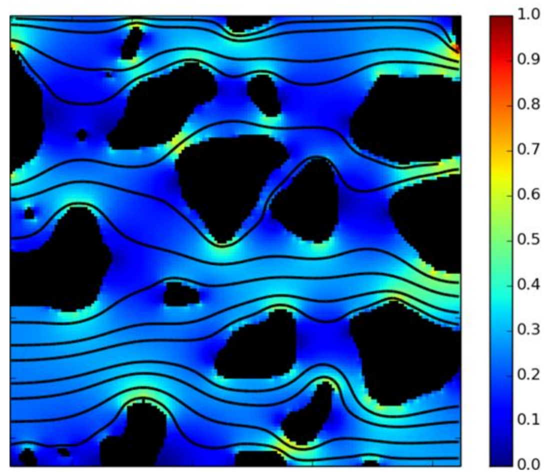

Figure 9. Lines indicating a set of electric field lines through the pore space, where the background colors represent the normalized magnitude of the electrostatic field $\|\mathbf{E}\| = \|\nabla\mathbf{\Phi}\|$.

$$A_e = \frac{L}{\int \frac{1}{A(x)} dx}. \tag{11}$$

This can be viewed as the effective cross-sectional area of the tube, and it is always smaller or equal to the average cross-sectional area of our tube with varying cross-sectional area. As the cross-sectional areas of the smallest pore throats dominate the integral in the denominator, the smallest pore throats are the limiting factor for the conductance. The pore volume of a tube with same resistance and constant cross-sectional area is less than the pore volume of the tube with variable cross-sectional area. Following (Owen, 1952), the fraction between these porosities is denoted the *constriction factor* C:

$$C = \frac{\bar{A}}{A_e} = \frac{1}{L}\int A(x)dx \frac{1}{L}\int \frac{1}{A(x)} dx, \tag{12}$$

where $\bar{A} = 1/L\int A(x)dx$ is the average cross-sectional area. For our single tube example we have $\sigma_0 = \sigma_w \phi / C$, thus we have $E_0 = 1/C$.

As the cross-sectional area of pore throats are typically much smaller than the cross sectional area of pore bodies, the equation for the constriction factor C above reveals that the resistance is dominated by the smallest or limiting pore throats. Following (Herrick and Kennedy, 1994), consider a *throat-tube* with constant cross-sectional area A_c equal the limiting constriction of the tube under consideration, as illustrated in Figure 12. The larger cross-sectional area inside the pores of the original tube increase conductance versus the corresponding throat-tube by a factor $d > 1$. Numerical simulations show that the conductance of the stream-tubes rocks is typically between 1 and 2 times larger than the conductance of the corresponding throat-tube (Herrick and Kennedy, 1994). As the increased conductivity by a factor d is in the same range as the decreased conductance due to tortuosity, these effects tend to cancel out. Thus the conductance of the tube is then approximated by the throat-tube with length equal the length of the sample, see lower illustration in Figure 12. The overall conductance of the rock can then be estimated as $\sigma_0 = \sigma_w \hat{A}_c / A$, where $\hat{A}_c$ is the total cross-sectional area of the limiting pore throats. In other words, a single straight tube with total cross-sectional area equal to the sum of the areas of all the smallest pore throats which limit conduction is a fair approximation of the conductance of the rock.

If we want to consider the effects of tortuosity and constrictions separately, then combining the above expressions for tortuosity and the constriction factor gives an estimate of the conductance as $\sigma_0 = \sigma_w \phi \tau^{-2} C^{-1}$ (Winsauer et al., 1952; Boyack and Gidding, 1962), which implies $E_0 = \tau^{-2} C^{-1}$. For simplified porous media it is possible to separate the pore geometry factor E_0 into the independent values of tortuosity and constriction factor. However, as pointed out by Wyllie in a discussion after the article of Owen (1952), both Owen and Winsauer et al. failed to resolve the fundamental difficulty of separating these quantities for realistic pore structures.

Effective values for tortuosity and constriction factor that give an exact expression $E_0 = \tau^{-2} C^{-1}$ for porous media in general were recently published by Berg (2012). Let P be the set of all electric field lines Γ in the porous medium Ω, then an effective tortuosity can be defined as

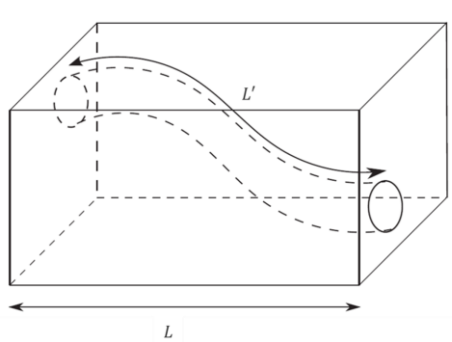

Figure 10. An idealized porous medium consisting of a single tortuous tube of length L' inside a cube of side-length L.

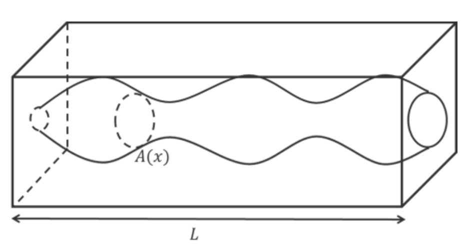

Figure 11. An idealized porous medium consisting of a single tube of varying cross-sectional area $\boldsymbol{A(x)}$ inside a cube of side-length $\boldsymbol{L}$.

$$\tau^2 = \left(\frac{1}{\Omega}\int_P \frac{1}{\tau(\Gamma)^2}\,d\Gamma\right)^{-1} \tag{13}$$

where $d\Gamma$ is the infinitesimal volume associated with the electric field line Γ. The tortuosity has a minimum value of 1, which is reached when all electric field lines are straight and have a length equal to the length of our porous medium. Longer electric field lines give a higher tortuosity, which reduces the efficiency of the porous medium to conduct electricity. Note that neither the value for the conductivity σ_w of the brine, nor the applied voltage drop $\Delta\Phi$ affects the tortuosity, thus the tortuosity is only dependent on the pore structure and the direction of the applied electric field.

When the electric current passes through a constriction, the current density $\mathbf{J}$ is increased. Variation in pore size thus translates into a variation in current density. For varying current density, energy is expended, and the effectiveness of the pore space to conduct flow is reduced.

Similar to the definition for a single tube above, we define the constriction factor $C(\Gamma)$ for an electric field line Γ of length l_Γ as

$$\begin{aligned} C(\Gamma) &= \frac{1}{l_\Gamma^2}\int_\Gamma \|\mathbf{E}(s)\|ds \int_\Gamma \frac{1}{\|\mathbf{E}(s)\|}ds \\ &= \frac{1}{l_\Gamma^2}\Delta\Phi \int_\Gamma \frac{1}{\|\mathbf{E}(s)\|}ds. \end{aligned} \tag{14}$$

The constriction factor C for the porous medium is then the current weighted average of the constriction factors for the electric field lines,

$$C = \frac{1}{I_t}\int_P C(\Gamma)dI_\Gamma \tag{15}$$

Here dI_Γ is the infinitesimal current associated with the electric field line Γ and I_t is total current through the porous medium.

The constriction factor has a minimal value of 1, reached when the electrostatic field is constant along each field line, e.g. when the pore volume is a straight tube. Larger variation in the electrostatic field due to changes in the pores cross-sectional area increases the constriction factor, and thereby reduces the conductance of the porous medium. As with the tortuosity, the constriction factor is also solely dependent on the pore structure and the direction of the voltage drop, and not on the porosity. Note also that both parameters are scale invariant.

For these effective values of the tortuosity and the constriction factor, it has been shown that $\sigma_0 = \sigma_w\phi\tau^{-2}C^{-1}$ (Berg, 2012). This gives an exact expression for our geometrical factor in terms of descriptors of the pore structure: $E_0 = \tau^{-2}C^{-1}$.

The Fontainebleau sandstone data revisited

Advances in imaging has made it possible for direct imaging of the pore structure in reservoir rocks on a resolution that allows for direct computation of electrical conductance with a high degree of accuracy. In combination with modeling of rock forming processes, this opens up new possibilities for understanding the controlling features for electrical conductance and transport in porous media in general.

We will now consider 7 digital rock models of the Fontainebleau sandstone, generated with the e-Core software (Berg, 2014). We used identical grain size distribution, sedimentation, compaction and diagenetic process parameters for the model constructions. Porosity values between 8% to 26% were obtained by only varying the amount of quartz cementation using a methodology introduced by (Pilotti, 2000). These models could therefore help to investigate the effect of quartz cementation, while all other parameters are kept constant.

On the grid representation of the models, we introduced an electrical potential $\Delta\Phi$ over two opposite end-planes of the sample and numerically solved the Laplace equation. On the resulting electrostatic potential field **E** we tracked electric field lines, and calculated the tortuosity and constriction factor as given by the equations introduced above. The results are plotted in Figure 13. The reason for plotting the inverse values, is that this is the way they occur in the expression for the geometrical factor $E_0 = \tau^{-2}C^{-1}$.

Observe that the trend of the inverse constriction factor crosses the *x*-axis at a positive porosity value. This indicates a possible percolation threshold for the constriction factor. The trend for the tortuosity values indicates a positive value at the apparent percolation threshold for the constriction factor, as expected.

The calculated geometrical factor $E_0 = \tau^{-2}C^{-1}$ is plotted versus porosity in Figure 14, together with two sets of experimental data. We have also plotted the product of the two trend lines in Figure 13 as the dashed curve in Figure 14. Note that this curve indicates a possible percolation threshold for the geometrical factor, being the percolation threshold of the constriction factor.

We observe a large spread in the experimental data compared to the trend of our calculated data. As the digital rock models (DRM) were created by changing only one parameter in the rock forming process, namely the amount of quartz cementation, it is as expected that their effective values follow a clear trend. The experimental data on the other hand contains rocks with varying grain size distribution, sorting etc., all of which creates a larger spread when plotted versus porosity. Still, as the Fontainebleau rock type is characterized by well sorted grains with varying degrees of quartz cementation, it is expected that the modeled and experimental data should follow similar trends. Inspection of Figure 14 shows that they clearly do.

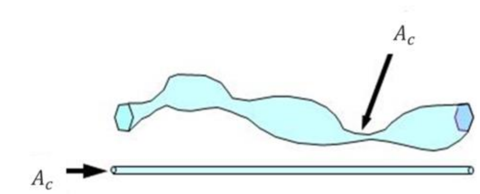

Figure 12: A simplified illustration of a stream-tube traversing a rock sample. The limiting constriction of this stream-tube is indicated by an arrow, and the corresponding throat-tube with length equal the length of the sample is illustrated below.

Summary and conclusion

The pioneers of formation evaluation in their efforts to construct a theoretical basis for the relationship connecting bulk rock resistivity to brine resistivity, porosity, and water saturation, recognized that pore geometry played an important role. However, they were not in agreement on how best to parameterize the effects of pore geometry. The earliest workers (Wyllie and Rose, 1950) mention the roles of variable brine cross sectional area and tortuosity, but thereafter in their paper fix the cross section of all pores as equal and treat tortuosity as the only parameter describing pore geometry. Their contemporary researchers (Winsauer et al., 1952; Owens, 1952) recognized the importance of variations in cross-sectional area, but these concerns did not lead to the general adoption of a pore-geometry model that contained pore constriction as a parameter. In models that contain tortuosity as the only pore geometric variable, the role of tortuosity is greatly exaggerated and its numerical values estimated are much higher than the actual tortuosity.

The adjustable parameters of the industry-standard interpretation paradigm, the repositories of pore and brine geometry in the Archie model *m*, *n*, and later, *a*, did not easily lend themselves to separation into a pair of factors, one for constrictivity and another for tortuosity.

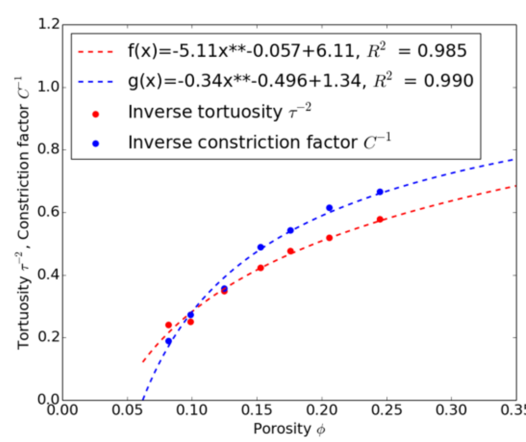

Figure 13: Plot of porosity versus the calculated values for inverse tortuosity squared and the inverse constriction factor.

A similar formulation was independently proposed by Herrick and Kennedy (1994). Further, by extending the results to fractional brine saturations, they formulated a complete alternative theory to Archie's law. Herrick and Kennedy (2009) called their model the geometrical factor theory.

Progress became possible when Herrick and Kennedy, (1993, 1994) invented their alternative model to Archie's law since it was based upon the physics of conduction in porous media. In this model, the pore geometry was intentionally designed to be a separate factor describing the departure of the geometry of a rock sample from the geometry of a right circular cylinder of the brine volume conducting current parallel to its axis. This separate factor is called the *geometrical factor*, denoted as E_0, and varies between 0 and 1. However, E_0 is still a single parameter used to describe the combination of all geometrical effects. Herrick and Kennedy (1994) suggested that the geometrical factor was composed of the effects of tortuosity and constrictions. Further progress became possible when the geometrical factor was expressed as a product of an expression for tortuosity and constrictivity in (Berg, 2012). Thus Berg was able to separate the effects of constriction C and tortuosity τ, and these two effects appear together as a product describing the geometrical factor in the Herrick and Kennedy model; viz. $E_0 = 1/(\tau^2 C)$.

This separation into independent factors of tortuosity and constrictivity into a brine geometry model, for the first time permits a proper weighting of the major controlling pore geometrical factors for formation resistivity. This richer parameterization of pore and brine geometry can lead to a fuller understanding of the controlling factors for electrical conductance, and may have implications for better understanding the permeability of conventional reservoir rocks.

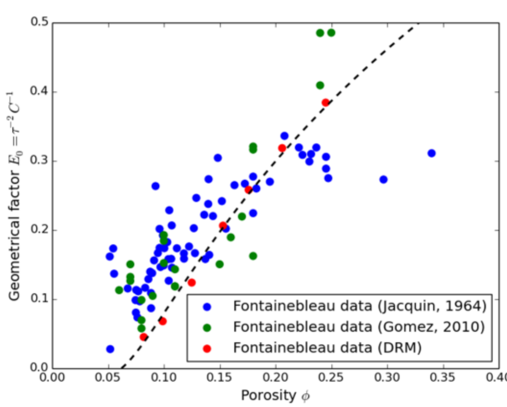

Figure 14: Plot of porosity versus geometrical factor for two sets of experimental data and for our digital rock models. The dashed line gives the product of the two curves plotted in Figure 13, indicating a trend for the digital rock models.

REFERENCES

Archie, G. E., 1942, The electrical resistivity log as an aid in determining some reservoir characteristics, *Transactions*, AIME, vol. 146.

Berg, C. F., 2012, Re-examining Archie's law: Conductance description by tortuosity and constriction, Physical Review E, vol. 86, DOI: 10.1103/PhysRevE.86.046314.

Berg, C. F., 2014, Permeability description by characteristic length, tortuosity, constriction and porosity, Transport in porous media 103 (3), pp. 381-400.

Boyack, James R, and Giddings, J. Calvin, 1963, Theory of Electrophoretic Mobility in Stabilized Media, Archives Of Biochemistry And Biophysics, vol. 100, pp. 16-25.

Bruggeman, D. A. G., 1935, Berechnung Verschiederner Physikalischer Konstanten von Hetarogenen Substanzen, Annalen der Physik, vol. 24, pp. 636-679.

Bussian, A. E., 1983, A comparison of shaly sand models, *Transactions* of the 24th SPWLA Annual Symposium, paper E.

Carman, P. C., 1937, "Fluid Flow Through Granular Beds", *Trans*. *Institution of Chem*. *Eng*., London, England, 15, pp. 150-166. (NNA. 890522. 0280).

Glover, P., 2009, What is the cementation exponent? A new interpretation, *The Leading Edge*, vol. 28, no. 1, p. 82-85.

Gomez, C.T., Dvorkin, J. and Vanorio, T., 2010, Laboratory measurements of porosity, permeability, resistivity, and velocity on Fontainebleau sandstones. *Geophysics*, vol 75, No. 6, E191–E204.

Guyod, Hubert, 1952, *Electric Well Logging Fundamentals*, Part 12, Fundamental Data for the Interpretation of Electric Logs, Well Instrument Developing Co., p. 76. (Probable original source is

Oil Weekly, Fundamental Data for the Interpretation of Electric Logs, Oct. 30, 1944.)

Hanai, T., 1962, Dielectric theory of the interfacial polarization for two-phase mixtures. *Bulletin of the Institute for Chemical Research*, Kyoto University (1962), vol. 39, no. 6. pp. 341-367.

Herrick, D. C. and W. D. Kennedy, 1993, Electrical efficiency: a pore geometric model for the electrical properties of rocks, *Transactions* of the 34th SPWLA Annual Logging Symposium June 13-16, paper HH.

Herrick, D. C. and W. D. Kennedy, 1994, Electrical efficiency-A pore geometric theory for interpreting the electrical properties of reservoir rocks, *Geophysics*, vol.59, No. 6, pp. 918-927.

Herrick, D. C. and W. D. Kennedy, 2009, A New Look at Electrical Conduction in Porous Media: A Physical Description of Rock Conductivity, *Transactions* of the 50th SPWLA Annual Logging Symposium June 21-24, The Woodlands, Texas.

Jacquin, C.G., 1964. Corrélation entre la perméabilite et les caractéristiques géométriques du grès de Fontainebleau. Rev. Inst. Fr. Pet. 19, 921.

Jakosky, J. J., Hopper, R. H., 1937, The Effect of Moisture on the Direct Current Resistivities of Oil Sands and Rocks, *Geophysics*., vol. 1, pp. 33-54.

Johnson, D. L., Koplik, J., Schwartz, L. M., New pore size parameter characterizing transport in porous media, *Physical Review Letters*, vol. 57, no. 20, 1986, pp. 2564-2567.

J. Kozeny, 1927, "Ueber kapillare Leitung des Wassers im Boden." Sitzungsber Akad. Wiss., Wien, 136(2a): 271-306.

Leverett, M. C., 1938, Flow of Oil-Water Mixtures through Unconsolidated Sands, *Trans*. AIME, pp. 149-171

Martin, M., Murray, G. H., Gillingham, W. J, 1938, Determination of the potential productivity of oil-bearing formations by resistivity measurements, *Geophysics*, vol. 3, pp. 258-272.

Monterond, B., Han, M., 2009, A connectivity model for the electrical conductivity of sandstone rocks, *Transactions* of the SPWLA 50th Annual Logging Symposium, paper FF.

Owen, J. E., 1952, The Resistivity Of A Fluid-filled Porous Body, Vol. 195, pp. 169-174, *Petroleum Transactions*, AIME. T.P. 3352.

Pilotti, Marco. "Reconstruction of clastic porous media." Transport in Porous Media 41.3 (2000): 359-364.

Schopper, Jurgen, 1966, A Theoretical Investigation on the Formation Factor/Permeability/Porosity Relationship using a Network Model, *Geophysical Prospecting*, vol. 14, pp. 301-341.

Sen, P.N.,1981, The dielectric and conductivity response of sedimentary rocks, *Transactions* of 55th Annual Fall Technical Conference and Exhibition of the SPE, Dallas, Texas, Sept. 21-24, SPE 9379.

Wyckoff, R. D., Botset, H. G., 1936, The Flow of Gas-Liquid Mixtures Through Unconsolidated Sands, *Physics*, vol. 7, pp. 325-345.

ACKNOWLEDGEMENT

The authors would like to thank the management of Statoil and Southwestern Energy for their support and permission to publish this article.

ABOUT THE AUTHORS

Carl Fredrik Berg is a reservoir engineer, working as a principal researcher in reservoir technology at Statoil. He received his Ph.D. in algebra from the Norwegian University of Science and Technology (NTNU) in 2006. After working as a lecturer at NTNU, he joined Statoil in 2007. His main research areas have been within digital rock modeling of flow in porous media and upscaling of transport processes.

David Herrick has mostly retired, but can't resist consulting and presenting his course on 'Pore Systems, Conductivity, Saturation and Permeability' with Yellowstone Petrophysics LLC. Dave is a petrophysicist with over 30 years experience in the petroleum industry. He was trained in chemistry and geochemistry at Indiana University (B.S.) and Penn State (Ph.D.). He has conducted research, training and technical service for Conoco, Amoco, Mobil and Baker Hughes in the areas of geochemistry, petrology and petrophysics. Dave has many publications and patents as well as having given numerous presentations and schools on petrophysics, resistivity interpretation, and the impact of pore geometry on permeability and conductivity.

David Kennedy studied physics at Georgia Tech and the University of Texas (Dallas) and geoscience at UTD and Berkeley. Work history includes Lieutenant of Infantry '67-'69, Schlumberger Field Engineer '73-'77, Arco log analyst '77-'78, World's Oldest Graduate Student '78-'86, Lockheed Missiles & Space Company '87-'88, Mobil Research '88-'92, Mobil Operations '92-'99, Exxon Research '00-'03, Exxon Operations '04-'07, BHI '08 '09, PathFinder '09-'13, Southwestern Energy '14-'16. Editor of Petrophysics Journal for 4 years, V.P. Publications for SPWLA for 4 years; SPWLA V.P. Technology '10. SPWLA leadership '13-'16 as President-Elect, President, and Past President. Inventor or coinventor on six patents and still counting, author or coauthor of 37 technical articles and still counting. Father of two, husband of one.